6th and 12th order vibration suppression of IPMSM by harmonic current injection

Y. Yamano[1] and K. Akatsu[2]

[1] Graduate School of Engineering Science ,Yokohama National University , Japan

[2] Yokohama National University , Faculty of Engineering , Division of Intelligent System Engineering , Japan

***Abstract*-- Torque ripple reduction in PMSM(Permanent Magnet Synchronous Motor) for EVs drive motors is one of the technologies that reduce vibration. Torque ripple reduction techniques require accurate torque ripple modeling and estimation of motor parameters considering magnetic saturation and magnet temperature variation. Existing approaches that consider magnetic saturation and magnet temperature variation are complex and difficult to implement. Therefore, this study uses phasers to represent torque ripples. This allowed us to represent the torque ripple geometrically and to determine the harmonic currents for torque ripple reduction in a simplified manner. This method is also extended to vibration suppression by measuring vibration using an acceleration sensor. In this paper, experimental results of 6th and 12th order vibration suppression are presented by using the determination method of the harmonic current commands. From these results, vibration can be suppressed by installing an acceleration sensor at locations where vibration is to be suppressed.**

***Index Terms*— PMSM , torque ripple , harmonic current injection ,vibration**

I. INTRODUCTION

PMSM(Permanent Magnet Synchronous Motor) is widely used for electric vehicles (EVs) drive motors because of their high efficiency, high power density, and high torque. With the increasing demand for EVs, lower vibration of PMSMs is required for further value addition. One of the vibration reduction technologies for PMSMs is torque ripple reduction.

Torque ripple reduction techniques can be divided into structural and control methods. Structural methods reduce torque ripple by optimizing the structure and geometry of the motor [1][2]. In contrast, control methods reduce torque ripple by injecting harmonic currents [3]-[5]. The control method is easier to implement than the structural method. Therefore, this paper focuses on torque ripple reduction technique by harmonic current injection.

Harmonic current control needs to determine the value of current, the detection methods include online determination of current command values using feedback (FB) [3]-[5] and offline determination of current command values using torque formula [6][7], feedforward (FF). The online determination method determines the compensation current by feeding back the instantaneous torque estimated from the rotor position and armature current and voltage. However, since FB control uses many FB values such as armature current and voltage, these noise signals can complicate the system [3][4]. Another disadvantage is the need to change the filter in response to speed fluctuations [5]. From the above, torque ripple reduction control basically requires FF control, and it is necessary to establish a method for determining the compensation current to reduce torque ripple. As FF control, a method to reduce torque ripple by determining a current command value for compensation from a torque ripple formula that considers magnet temperature variation [6]. However, in [6], there is the disadvantage that the search for the current command value for compensation is troublesome because it is necessary to create a current map for each constant magnet temperature and correct the current command value for compensation. In addition, the current-flux characteristics of the motor may be approximated linearly, with no consideration given to nonlinearities such as magnetic saturation [7]. Therefore, there is a problem of deterioration of the torque estimation system. From the above, it is essential for FF control of harmonic current injection to consider magnetic saturation, to represent complex torque behavior in a simplified manner, and to determine harmonic current command values in a simplified manner.

Therefore, authors have reported a detection method of the harmonic current command in [8]. The method has shown that the torque ripple can be drawn on a complex vector plane, and the complex behavior of the torque ripple characteristics can be expressed very concisely in terms of phase differences. Furthermore, they have shown that the characteristics of the torque ripple with the addition of harmonic currents draw a circular trajectory on the plane, and they have proposed the method to geometrically determine the current reference to reduce the torque ripple using this trajectory. The advantage of this method is that by geometrically determining the current reference on a complex vector plane, the compensation current reference can be determined without using complex behavior motor parameters. While the [8] suppressed up to 6th order torque ripple, this research expanded the method to 6th and 12th order torque ripple and vibration suppression. In this paper,6th and 12th order vibration suppression are presented in the experiment. These results show that vibrations can be easily suppressed by installing accelerometers at the locations where vibration should be suppressed.

II. METHOD OF DETERMINING CURRENT COMMAND VALUES FOR COMPENSATION [8]

A. Principle of torque ripple generation

Torque is generated by the outer product of the current and armature flux. Since the current and armature flux are three-phase AC, harmonic components are generated at 5, 7, 11, 13... and 6n±1 (n=positive integer) Therefore, the torque ripple, which is the harmonic component of torque, is generated by the outer product of the fundamental current and the harmonic flux or the fundamental flux and the harmonic current. From this, it is generated at the 6nth order.

The 6nth order torque ripple generated by the outer product of the fundamental current and the 6n±1th order harmonic flux is the torque ripple to be suppressed. In contrast, the torque ripple can also be generated by the outer product of the fundamental flux and the 6n±1th order harmonic current. This torque ripple is used as the compensation torque ripple to cancel the torque ripple to be suppressed. 6n±1 order currents can both generate the compensation torque ripple, but since the higher the order, the higher the frequency of the current, the 6n-1 order compensation harmonic currents are used to cancel the 6n torque ripple due to the inverter's carrier frequency. The 6nth order torque ripple is canceled out by using the 6n-1 th order compensating harmonic current due to the inverter carrier frequency.

B. Expression of torque ripple on phasor

The torque ripple expression in phasors is shown below. 6nth order torque ripple is expressed as follow:

$$T_{6n} = |T_{6n}| exp\{j(6n\theta_e + \angle T_{6n})\} \quad (1)$$

Where, $|T_{6n}|$: Amplitude of 6nth order torque ripple, $\angle T_{6n}$: phase of 6nth order torque ripple.

From (1), it is possible to express the torque ripple if the phase and amplitude of the torque ripple are known. Fig. 1 shows 6nth order torque ripple on the phasor. From Fig. 1 and (1), if the phase and amplitude are known, it is possible to express the torque ripple on the phaser.

C. Behavior on the phasor

The torque ripple to be suppressed generated by the fundamental current and the torque ripple for compensation generated by the harmonic current are represented on the phasors. Fig. 2(a) shows the 6nth order torque ripple of the suppression target when the fundamental current is superimposed on the phase. Next, Fig. 2(b) shows the behavior of the 6n-1th order harmonic current superimposed on the fundamental current with a different phase. From Fig. 2(b), the torque ripple caused by the harmonic currents on the phasor draws a circular trajectory centered at the end point of the torque ripple caused by the fundamental current and synchronized with the phase of the superimposed harmonic currents. Next, Fig. 2(c) shows the behavior of the 6n-1th harmonic currents superimposed on the fundamental currents with different phase amplitudes. From Fig. 2(c), the torque ripple caused by the harmonic currents on the phasor is proportional to the amplitude of the superimposed harmonic currents and the radius of the circle centered at

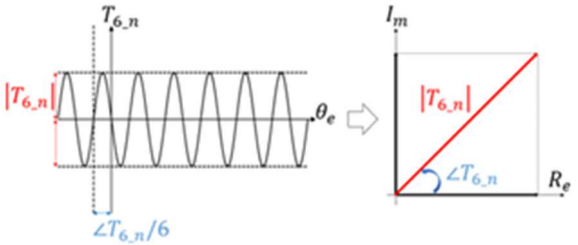

Fig. 1 Expression of the torque ripple on the phasor.

the end point of the torque ripple caused by the fundamental currents. Fig. 2(d) shows the behavior of the harmonic currents when their phase and amplitude are optimized. Centered on the torque ripple to be suppressed, the phase of the circle is synchronized with the phase of the current, and the amplitude of the circle is proportional to the amplitude of the current.

D. Harmonic current determination method for torque ripple reduction

From Fig. 2(d), on the torque ripple phasor, the distance from the origin indicates the magnitude of the torque ripple, and when at the origin, the torque ripple is zero. The conditions for reducing the torque ripple are shown in equations (2) and (3).

$$|T_{harm}| = |T_{fund}| \quad (2)$$

$$\angle T_{harm} = \angle T_{harm_0} + \angle I_{harm} = \angle T_{fund} + 180\text{deg.} \quad (3)$$

Where, $|T_{harm}|$: Amplitude of compensating torque ripple caused by harmonic currents, $|T_{fund}|$: Amplitude of torque ripple to be suppressed caused by fundamental current, $\angle T_{harm_0}$: Phase of torque ripple when harmonic currents of phase 0 deg. are superimposed, $\angle I_{harm}$:Ha rmonic current phase, $\angle T_{fund}$: Phase of torque ripple to be suppressed caused by fundamental current.

From (2) and (3), to reduce the torque ripple, a compensating torque ripple can be generated by the harmonic current , the same amplitude and opposite phase as the torque ripple to be suppressed caused by the fundamental current. The compensation torque ripple caused by the harmonic current on the phasor shows a circular behavior, and the compensation torque ripple can be shown by (4) and (5).

$$|T_{harm}| = c_{harm} \times |I_{harm}| \quad (4)$$

$$\angle T_{harm} = \angle I_{harm} + \angle T_{harm\_0} \quad (5)$$

Where, c_{harm} : Torque ripple coefficient caused by harmonic current, $|I_{harm}|$:Amplitude of harmonic current.

Therefore, from (2)-(5), the harmonic currents for torque ripple reduction can be shown by (6) and (7).

$$|I_c| = \frac{|T_{fund}|}{c_{harm}} \quad (6)$$

$$\angle I_c = \angle T_{fund} - \angle T_{harm_0} + 180\text{deg.} \quad (7)$$

Where, $|I_c|$:current command value of amplitude , $\angle I_c$: current command value of phase. From (6) and (7), the only parameters required are the amplitude and phase of the torque ripple to be suppressed caused by the

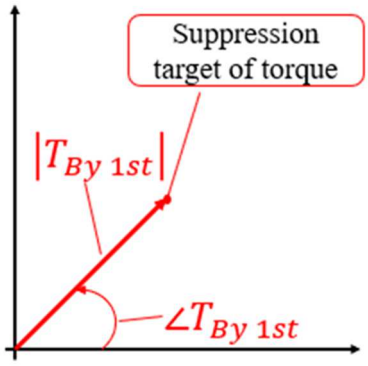

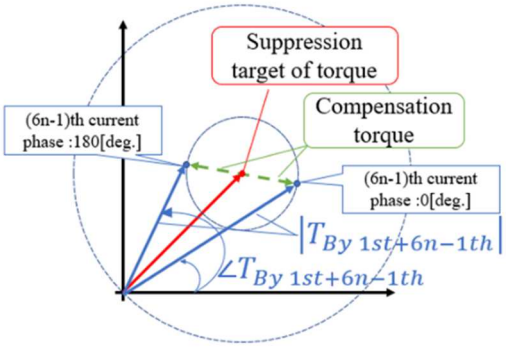

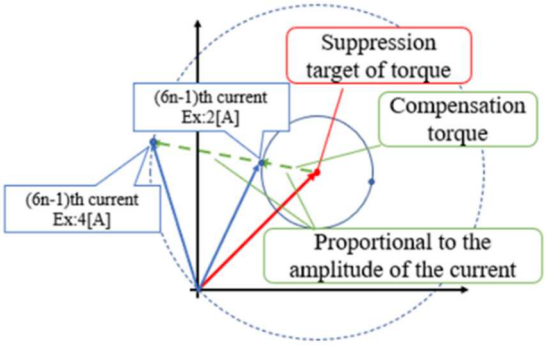

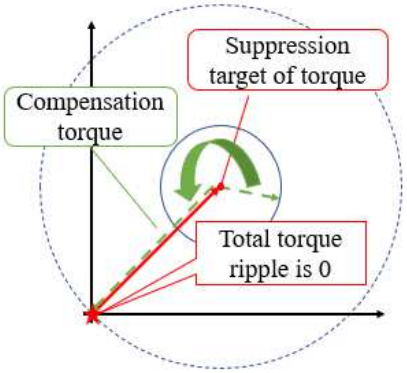

(c) Behavior when superimposed different amplitude of 5th order current.

(d) Behavior when adjusting phase and amplitude of 5th order current.

Fig. 2 Conceptual diagram of torque ripple suppression.

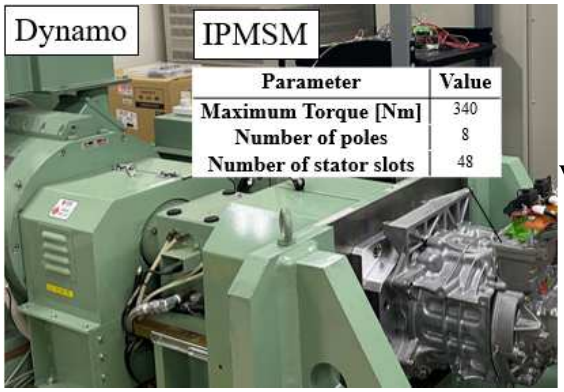

Fig. 3 Experimental environment.

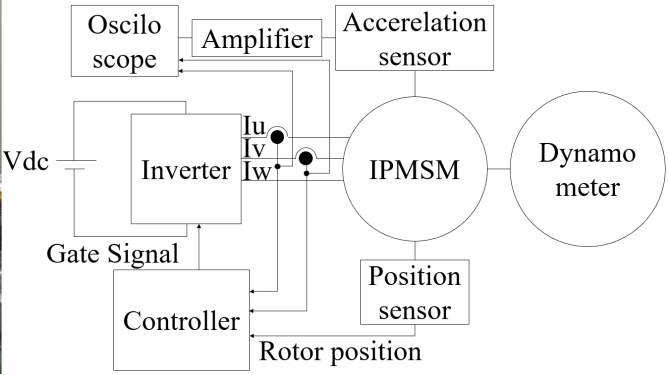

Fig.4 Experimental environment block diagram.

fundamental current and the amplitude and phase of the torque ripple for compensation caused by the harmonic currents. Harmonic current command values can be determined simply.

E. Expansion to vibration suppression

Extend the method of [8] to vibration suppression. Torque ripple suppression required the use of a torque meter. Since a torque meter cannot measure the ripple due to its accuracy and error, an acceleration sensor is used to measure the vibration. So, vibration is measured using an acceleration sensor, and FFT (Fast Fourier Transform) is performed to extract the phase and amplitude of the vibration. From this, harmonic current command values can be calculated in the same way as for torque ripple.

III. EXPERIMENT

A. Experiment environment

In the proposed method, the reduction of torque ripple is extended to vibration suppression. Then, experimental results of suppression of 6th and 12th order vibrations at the same time are obtained. Fig. 3 shows the experimental environment. Fig.4 shows block diagram of the experimental environment. The motor used in the experiment is an IPMSM for EV traction motor. Fig.5 shows the acceleration sensor and measurement point. Select the points among the measurement points where 6th and 12th order vibrations are pronounced. Then, TABLE I shows the acceleration sensor specification. The measured

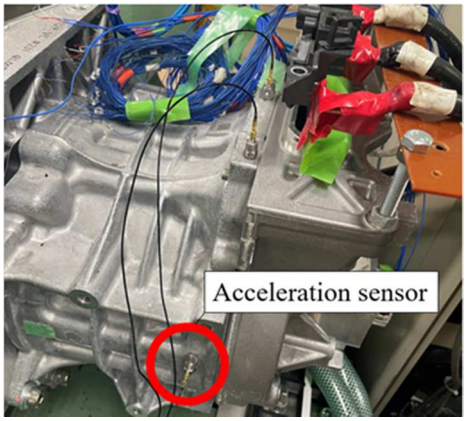

Fig. 5 Acceleration sensor.

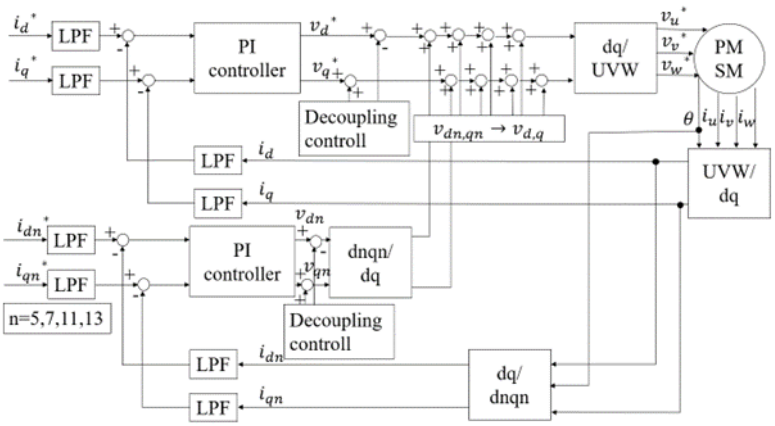

Fig.6 Control block diagram.

vibration is FFT, and a phasor is created in the same way as for the torque ripple, and a current command value is created. TABLE II shows the experimental condition. A control block diagram is shown in Fig.6. Control is performed as shown in Fig. 6.

B. Experimental result

Fig. 7 shows the measured vibration acceleration and the U-phase current when only the fundamental current is added. U-phase current is used for a position reference. It is measured with an oscilloscope and input as a trigger for the vibration acceleration signal. Fig. 7 shows that 6th and 12th order vibrations are more pronounced The FFT results in Fig. 7 show that the phase and amplitude of 6th vibration caused by fundamental current are (8) and (9)

$$|T_{fund}| = 0.224\ [\mathrm{m/s^2}] \quad (8)$$

$$\angle T_{fund} = 140.3\ [\mathrm{deg.}] \quad (9)$$

TABLE I. Acceleration sensor specification

Parameter	Value
Manufacture	ONOSOKKI
Model number	NP-3412
Sensitivity [mV]	1.0
Resonance frequency [kHz]	40
Range of frequency [Hz]	2-8,000

TABLE II. Experimental conditions

Parameter	Value	
	5th command value creation	5th command value injection
Rotational speed [min^{-1}]	2000	
Carrier frequency [kHz]	20	
DC voltage [V]	365	
1st current [A]	72	
1st current phase [deg.]	30	
5th current [A]	3,4	1.7
5th current phase [deg.]	0-330(per 30)	268.6
7th current [A]	0	
7th current phase [deg.]	0	

C. 5th order current command value superimposition result (vibration acceleration FFT)

Next, the 5th harmonic current is superimposed by changing the amplitude and phase. Fig. 8 shows the result of 5th harmonic current superposition. Fig. 8 confirms that the vibration also shows a circular behavior on the phaser. When 5th order current of phase 0 deg. and amplitude 3 A is flowed, the phase and amplitude of the 6th order vibration are (10) and (11).

$$|T_{harm_{5th\_0}}| = 0.224\ [\mathrm{m/s^2}] \quad (10)$$

$$\angle T_{harm5th\_0} = 51.7\ [\mathrm{deg.}] \quad (11)$$

Where $|T_{harm5th\_0}|$: Amplitude of compensating torque ripple caused by 5th harmonic current(0deg.) , $\angle T_{harm5th\_0}$: Phase of compensating torque ripple caused by 5th harmonic current (0deg.) . Then, the superimposed 5th harmonic current command value is computed from (6)-(11). These can be expressed by (12)-(14).

$$c_{harm} = \frac{|T_{harm5th\_0}|}{|I_{harm}|} = \frac{0.39}{3} = 0.13 \quad (12)$$

$$|I_{c5}| = \frac{|T_{fund}|}{c_{harm}} = \frac{0.224}{0.13} = 1.7\ [\mathrm{A}] \quad (13)$$

$$\angle I_{c5} = \angle T_{fund} - \angle T_{harm_{5th_0}} + 180$$
$$= 140.3 - 51.7 + 180 = 268.6\ [\mathrm{deg.}] \quad (14)$$

So, the superimposed 5th harmonic current command value is determined to be 1.7A and 268.6deg. Fig. 8(b),(c) shows the result of superimposing the current command value and 84.7% of the 6th order vibration is suppressed by superimposing the 5th order current. (This is the average suppression ratio of three measurements.)

Similarly, the 11th order command values are created and superimposed. Fig. 9(a) shows the result of superimposing the created phasor and Fig. 9(b), (c)shows the result of superimposing the command values. Fig. 9(c) shows that 80.4% of the 12th order vibration is suppressed by superimposing the 11th order current. (This is the average suppression ratio of three measurements.)

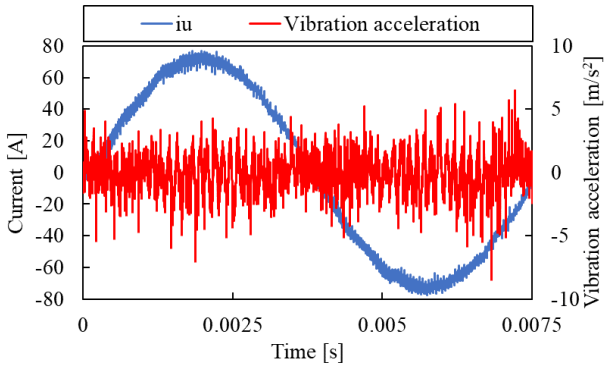

(a) Vibration acceleration and current.

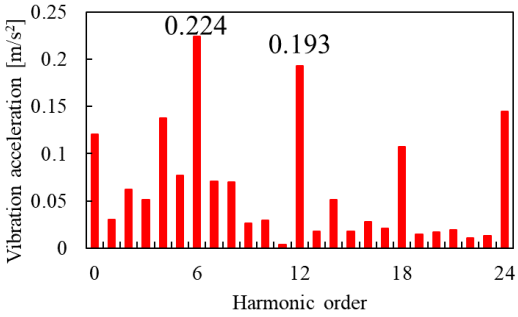

(b) FFT result of vibration acceleration.

Fig. 8 Measured vibration acceleration and the U-phase current.

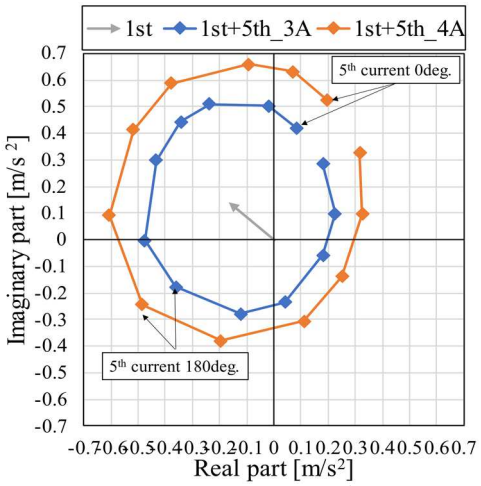

(a) Phasor of vibration acceleration by 5th order current.

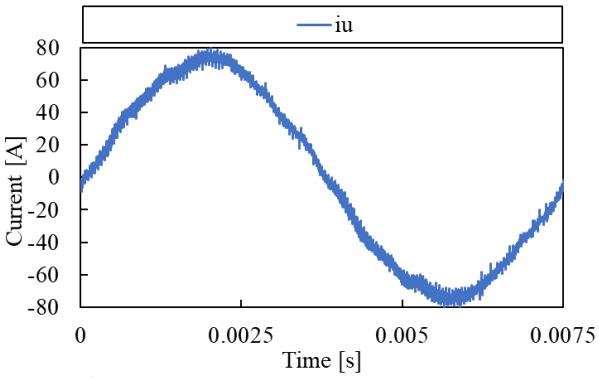

(b) 5th order current command value superimposition result(current).

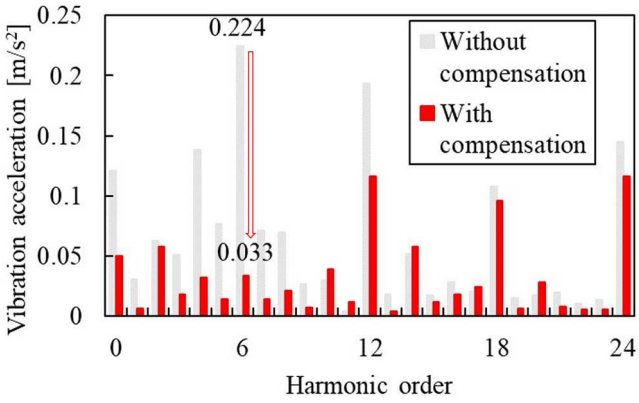

(c) 5th order current command value superimposition result (vibration acceleration FFT).

Fig. 9 Vibration behavior with 5th order current injection

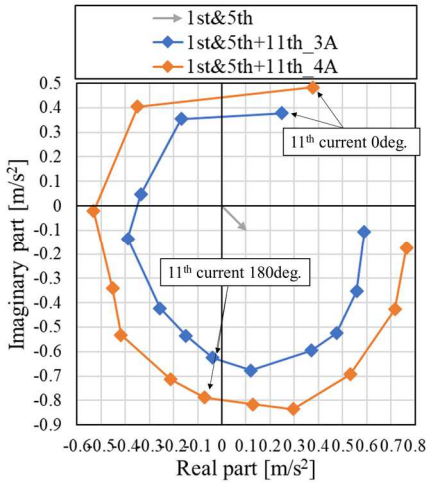

(a) Phasor of vibration acceleration by 5th order current.

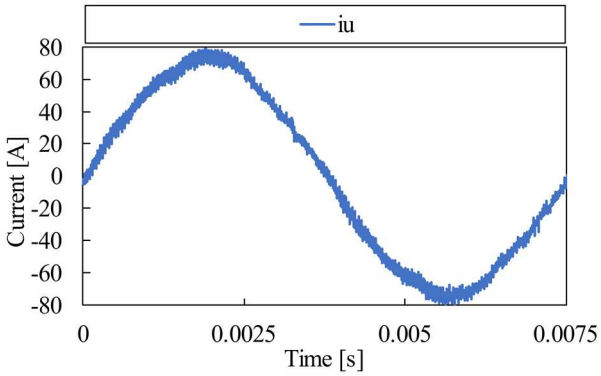

(b) 11th order current command value superimposition result(current).

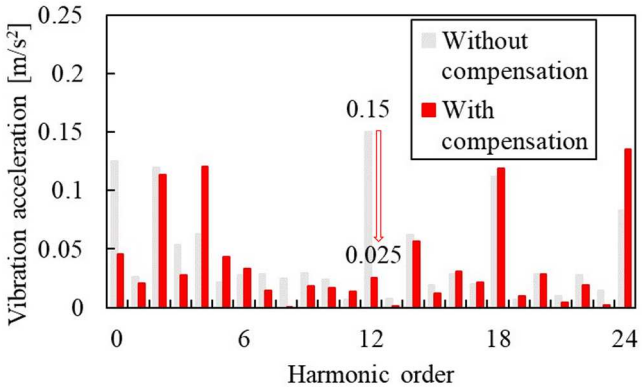

(c) 11th order current command value superimposition result (vibration acceleration FFT).

Fig.10 Vibration behavior with 11th order current injection.

IV. Conclusion

In this paper, vibration suppression is performed by a simple current command value determination method using a phaser. By installing an acceleration sensor, the 6th order vibration is suppressed by 84.7% and the 12th order vibration by 80.4%. From this result, vibration can be suppressed by installing an acceleration sensor at locations where vibration is to be suppressed. Future plans include expanding the control area of the proposed method to high speed area. Vibration can be suppressed even when the rotation speed is increased.

[1] C. Peng, D. Wang, B. Wang, J. Li, C. Xu and X. Wang, "Torque Ripple and Electromagnetic Vibration Suppression in Permanent Magnet Synchronous Motor Using Segmented Rotor With Different Pole Widths," in *IEEE Transactions on Magnetics*, vol. 58, no. 9, pp. 1-5, Sept. 2022.

[2] T. Soeda and H. Haga, "Suppression to Radial Force and Torque Ripple of Concentrated PMSM with Double Independent Three-Phase Windings," *2020 23rd International Conference on Electrical Machines and Systems (ICEMS)*, Hamamatsu, Japan, 2020, pp. 509-514

[3] L. Yan, Y. Liao, H. Lin and J. Sun, "Torque ripple suppression of permanent magnet synchronous machines by minimal harmonic current injection," IET Power Electron., vol. 12, no. 6, pp. 1368-1375, 2019.

[4] Yuki Terayama, Nobukazu Hoshi, "Torque Ripple Suppression Control in PMSM Using Estimated Harmonic Component of Flux Linkage Considering Magnetic Saturation", *IEEJ Transactions on Industry Applications*, vol.141, no.4, pp.366, 2021.

[5] J. Qu, J. Jatskevich, C. Zhang and S. Zhang, "Torque Ripple Reduction Method for Permanent Magnet Synchronous Machine Drives With Novel Harmonic Current Control," in *IEEE Transactions on Energy Conversion*, vol. 36, no. 3, pp. 2502-2513, Sept. 2021,

[6] G. Feng, C. Lai, K. L. V. Iyer and N. C. Kar, "Torque ripple modeling and minimization for PMSM drives with consideration of magnet temperature variation," *2016 XXII International Conference on Electrical Machines (ICEM)*, 2016, pp. 612-618 .

[7] N . Nakao , K . Tobari , T. Sugino , Y. Ito, M.Mishima and D.Maeda,"Torque Ripple Suppression Control for PMSMs using Feedforward Compensation and Online Parameter Estimation" *IEEJ Transactions on Industry*

[8] T. Nishio, Y. Ryosuke, K. Masahiko and K. Akatsu, "A Method of Torque Ripple Reduction by Using Harmonic Current Injection in PMSM," 2019 IEEE 4th International Future Energy Electronics Conference (IFEEC), 2019, pp. 1-5.